ACADEMIC PRESS

Available online at www.sciencedirect.com

SCIENCE DIRECT®

Journal of Computational Physics 186 (2003) 652–665

JOURNAL OF COMPUTATIONAL PHYSICS

www.elsevier.com/locate/jcp

A digital filter based generation of inflow data for spatially developing direct numerical or large eddy simulations

M. Klein *, A. Sadiki, J. Janicka

Technische Universität Darmstadt, FG Energie- und Kraftwerkstechnik, Petersenstrasse 30, 64287 Darmstadt, Germany

Received 22 May 2002; received in revised form 28 January 2003; accepted 10 February 2003

Abstract

In contrast to time-evolving turbulence, direct numerical or large eddy simulations of spatially inhomogeneous flows require turbulent inflow boundary conditions, that make the results strongly influenced by the velocity profiles to be prescribed. This paper aims to present a new approach for generating artificial velocity data which reproduces first and second order one point statistics as well as a locally given autocorrelation function. The method appears to be simple, flexible and more accurate than most of the existing methods. This is demonstrated in two cases. First, direct numerical simulations of planar turbulent jets in the Reynolds number range from 1000 to 6000 are performed. Because of the importance of the primary breakup mechanism of a liquid jet in which inflow influences are evident, the new procedure is secondly used, to study atomization in dependence of the flow inside the nozzle by means of a Volume of Fluid scheme.

Keywords: Digital filter; Inflow generation; Inflow boundary conditions; DNS

1. Introduction

It is well recognized that besides the mathematical model and the numerical scheme, properly chosen boundary conditions are of great importance in view of a good representation of a physical system. From a mathematical point of view the imposition of exact boundary and initial values is a necessary condition for a unique solution of the set of partial differential equations to be solved. For the case of turbulent flows, in contrast to time-evolving turbulence, direct numerical or large eddy simulations of spatially inhomogeneous flows require turbulent boundary conditions. This fact makes the results strongly influenced by the velocity data prescribed at the inflow and constitutes a vicious circle: Turbulence has to be prescribed at the inflow in order to simulate turbulence. It depends on the flow and the question under consideration how

* Corresponding author.

E-mail addresses: kleinm@hrzpub.tu-darmstadt.de (M. Klein), sadiki@ekt.tu-darmstadt.de (A. Sadiki), janicka@ekt.tu-darmstadt.de (J. Janicka).

0021-9991/03/$ - see front matter
doi:10.1016/S0021-9991(03)00090-1

far-reaching the consequences are. As demonstrated in [1–3], as well as in [4] the results of the direct numerical simulation of a plane jet, a spatially developing boundary layer or the primary breakup of a liquid sheet are very sensitive to the inflow conditions.

A lot of investigations have been carried out and different methods, to break through the above described vicious circle (see also [4,5]), have been attempted. A basic rule is to design the computational domain so that all boundaries are located far from the area of interest. Therefore the boundary problem is partially a problem of computing time, but there are also imaginable flow configurations where the problem cannot be solved by extending the computational domain, for example very complex or very short nozzles.

A most elegant way to avoid this problem is the use of periodic boundary conditions, which is unfortunately restricted to a few geometries like the channel flow. Spalart [6] was able to extend the area of application to a turbulent boundary layer by using coordinate transformations. However, according to [5] Spalart's approach is restricted to flows whose mean streamwise variation is small compared to the transverse variation. A further disadvantage is the complexity of the method. Therefore, Lund et al. [4] extended Spalart's idea: An auxiliary simulation which produces its own inflow conditions by rescaling the velocity field from a downstream location and re-introducing at the inflow, is used to extract instantaneous planes of velocity. Therefore, one can speak from semi-periodic boundary conditions combined with a separate simulation. A discussion to what extend periodic boundary conditions disturb large scale structures in the computational domain can be found in [7].

Closely connected to this technique are simulations which obtain inflow data from an auxiliary simulation. For example in the case of a nozzle with a high length to diameter ratio, the flow can be regarded as a fully turbulent channel flow and therefore be very well described by a channel flow simulation. This procedure produces very good inflow conditions but remains restricted to some simple geometries and implies additional computational effort. All the above mentioned methods are very satisfying from a physical point of view, but often are not practicable. In the case of a plane jet a contraction nozzle is often used experimentally, which produces a flat velocity and fluctuation profile. Theoretically it would be possible to perform a DNS of this geometry, but the question would arise which boundary conditions should be used for this simulation.

In view to generate boundary conditions only from the knowledge of the flow geometry and eventually some experimental data, one possibility is, to extract the most amplified modes based on a solution of the Orr–Sommerfeld equation, and to prescribe them at the inflow, as shown for example in [8]. However the derivation of the Orr–Sommerfeld equation is based on a lot of simplifications, which are seldom fulfilled in reality, and the flow field is not turbulent. On the other hand the method is well suited for the examination of transition, because it is important that transition is not only triggered by roundoff errors of the numerical scheme.

The simplest way to generate turbulent inflow data is to take a mean velocity profile with superimposed random fluctuations. Fig. 1 shows that this is not a very good method. For random data generated by standard procedures the energy of the signal is equally distributed over the whole wavenumber range, that means the spectrum is approximately a horizontal line. Therefore, due to a lack of energy in the low wave number range, the pseudo turbulence is immediately damped to zero, and the result is identical with a laminar inflow. An improvement of this method, first presented by Lee et al. [9], will be discussed in Section 4 followed by a new proposal which is the object of this paper.

Intermediate in computational cost is the method by Bonnet et al. [10]. They combine the Proper Orthogonal Decomposition with a Linear Stochastic Estimation to generate a realistic velocity profile by using expensively measured time series and correlation functions. Their method has been successfully used for the simulation of a mixing layer.

If periodic boundary conditions are excluded for reasons of the flow geometry and if it is not possible to perform an auxiliary simulation, one finds in the situation to generate artificial inflow velocity profiles, which should capture the essential properties of the flow.

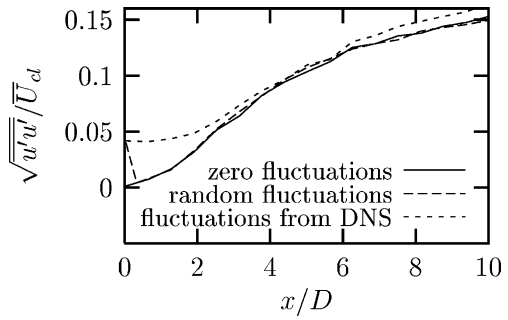

Fig. 1. Influence of conventional inflow boundary conditions on the simulation of a plane jet. Comparison between inflow with zero fluctuations, random fluctuations and fluctuations from an external channel flow DNS.

In order to present the methodology used in this work, we recall in the following section the governing equations and the numerical technique needed for the simulations. The new method of generation of artificial inflow data is then presented in Section 4, after shortly outlining the conventional approach in Section 3. Some applications are presented and discussed in Section 5. They consist of a simulation of a monophasic plane jet and a (two-dimensional) simulation of a water film ejected into air. Finally some conclusions will close the paper.

2. Governing equations and numerical technique

For the points to be addressed, we deal with the following set of conservation equations in their instantaneous, local form. The continuity equation in an incompressible formulation

$$\frac{\partial u_i}{\partial x_i} = 0 \tag{1}$$

and the Navier–Stokes equation

$$\frac{\partial}{\partial t}(\rho u_i) = -\frac{\partial}{\partial x_j}(\rho u_i u_j) + \frac{\partial}{\partial x_j}\mu\left(\frac{\partial u_i}{\partial x_j} + \frac{\partial u_j}{\partial x_i}\right) - \frac{\partial p}{\partial x_i} + \frac{\partial T_{s(ij)}}{\partial x_j}. \tag{2}$$

As usual ρ denotes the density and μ the molecular viscosity. In Eq. (2) the consideration of two phase flows is included through the interfacial stress tensor $T_{s(ij)}$ to be modeled below. The interface between the two immiscible fluids is implicitly given by the volume fraction F which is advected by the following equation

$$\frac{\partial F}{\partial t} + u_i \frac{\partial F}{\partial x_i} = 0. \tag{3}$$

At the interface, continuity of fluid velocity is assumed, that means the limiting values of velocity $\mathbf{u}_L$ and $\mathbf{u}_G$ are identical. In (2) the interfacial tension stress acting between the two fluid phases is usually modeled by considering only the inviscid term and assuming it to be a constant [11]

$$\boldsymbol{T}_s = \sigma(\boldsymbol{I} - \boldsymbol{nn})\delta_s \quad \text{and} \quad \nabla \cdot \boldsymbol{T}_s = 2\sigma\kappa\boldsymbol{n}\delta_s, \tag{4}$$

where σ denotes the surface tension, $\boldsymbol{n}$ the unit normal on the surface, κ the mean curvature, δ_s a Dirac function concentrated on the surface and $\boldsymbol{I}$ the unit tensor. An extension of this formulation, in which a surface deformation rate has been taken into account, may be found in [12].

Eqs. (1) and (2) are solved, using a finite volume technique on a cartesian mesh. The variables are located on a staggered grid. For spatial discretization central differences or especially for high density ratios a TVD scheme is used. Temporal discretization is an explicit third order Runge–Kutta-method. The Poisson equation is inverted with a direct fast elliptic solver. In the case of a two phase flow, a Multigrid Solver with Galerkin coarse grid approximation is used.

To account for the advection of the interface in the frame of two phase flows, a Volume-of-Fluid scheme with PLIC interface reconstruction was used following [13,14], so that droplet formation and ejection away from the liquid jet can be captured.

At the outflow Neumann boundary conditions for the velocity and the pressure are prescribed. Setting the pressure to zero at the top and the bottom boundaries and interpolating the tangential velocities constantly allows for mass entrainment. Periodic boundary conditions are applied in the homogenous direction. The generation of inflow conditions is explained in Section 4.

While in DNS the numerical resolution is sufficiently fine so as to resolve all scales of motion and scalar that carry significant energy, in the large eddy simulation approach one only resolves those eddies that are large enough to contain information about the geometry and dynamics of the specific problem under investigation, and regards all structures on a smaller scale as "universal" following the viewpoint of Kolmogorov. The LES equations are therefore derived by applying a filter function to Eqs. (1)–(3). This filtering process separates out the effects of the highly geometry dependent large scales from the more universal small scales to be modeled by a subgrid scale model. For details, see [15]. Therefore, these large scales are also inhomogeneous and directly affected by the boundary conditions.

3. Conventional generation of inflow conditions

The conventional way to generate turbulent inflow data is to take a mean velocity profile with superimposed fluctuations. Using the numerical technique described in Section 2 we performed in [16] a simulation of a plane jet at Reynolds numbers varying in the range from 1000 to 6000. Although the results compared well with experimental data for self similarity profiles, the jet spreading rate was underpredicted by approximately 20%. The most probable explanation for this discrepancy seemed to be the use of non-realistic inflow conditions.

In Fig. 1 we compare the axial evolution of the longitudinal velocity fluctuations from three simulations, which differ only in the inflow boundary conditions. A mean velocity profile from a channel flow simulations has been used with superimposed: (1) zero fluctuations, (2) random fluctuations and (3) fluctuations from an external channel flow DNS.

It can be seen that due to a lack of energy in the low wave number range, the pseudo turbulence is immediately damped to zero, and the result is identical with a laminar inflow. Therefore this is not a very good method for generating inflow data. This explains a certain independence of the fluctuation level on the simulation results, when using 'white noise' fluctuations. In consideration of this fact the choice of laminar inflow conditions seems to be superior to the random fluctuation approach. Additionally if an iterative solver is used, the number of iterations can be reduced dramatically, see for example [17]. The use of real turbulence, e.g. from an auxiliary simulation, at the inflow shows a complete different behavior. In this case the fluctuation level is maintained and increases up to the end of the potential core where the shear layer has penetrated into the jet up to the centerline. Unfortunately the spreading rate remained still considerably underpredicted.

In the framework of two phase flow, atomization of liquid jets is of fundamental interest for the automotive industry, gas turbines, medicine, agriculture, etc. Several mechanisms for the disintegration of turbulent jets have been proposed by various workers (see [18]). However, the physical phenomena leading to the disintegration of jets are still not very well understood. Examples include the assertion that atom-

ization is due to aerodynamic interaction between the liquid and the gas, leading to unstable wave growth on the jet surface, or alternatively that the breakup process starts within the nozzle itself and is strongly influenced by turbulence. So the influence of the inflow conditions is closely connected to the influence of the turbulence inside the nozzle on the primary jet breakup, which is for itself an outstanding question. In the following we present a new approach to investigate these aspects and to improve the jet spread prediction.

4. Improved approaches to generate artificial inflow data

An usual approach for the generation of artificial inflow data is to produce a velocity signal which has certain statistical properties, which may for example be known from experimental data. Such quantities are mean values, fluctuations and cross correlations, higher order moments, length and time scales, energy spectra, etc. Such a procedure can be splitted in two parts:

1. First a provisional three-dimensional signal $\mathscr{U}_i$ is generated for each velocity component which possesses a prescribed two point statistic (length scale, energy spectra). If there would only be the need to obtain homogenous turbulence the procedure could stop here.
2. If cross correlations between the different velocity components have to be taken into account a method proposed by Lund et al. [4] can be used. First define $\mathscr{U}_i$ so that $\overline{\mathscr{U}_i} = 0, \overline{\mathscr{U}_i \mathscr{U}_j} = \delta_{ij}$ and then perform the following transformation: $u_i = \bar{u}_i + a_{ij}\,\mathscr{U}_j$ with

$$(a_{ij}) = \begin{pmatrix} (R_{11})^{1/2} & 0 & 0 \\ R_{21}/a_{11} & (R_{22} - a_{21}^2)^{1/2} & 0 \\ R_{31}/a_{11} & (R_{32} - a_{21}a_{31})/a_{22} & \left(R_{33} - a_{31}^2 - a_{32}^2\right)^{1/2} \end{pmatrix}. \tag{5}$$

Here $\overline{(\cdot)}$ denotes an appropriate averaging procedure, R_{ij} the correlation tensor which may be known from experimental data and u_i the finally needed velocity signal.

A method for solving part 1 has first been proposed by Lee et al. [9]. The idea is based on an inverse Fourier Transform and will be illustrated by a one-dimensional example.

4.1. Inverse Fourier transform by Lee et al. [9]

Let's suppose a discrete signal u_k is given in physical space, then the Fourier Transform defines uniquely the corresponding signal U_n in wave number space.

$$u_k = \frac{1}{N}\sum_{n=0}^{N-1} U_n \mathrm{e}^{2\pi \mathrm{i} k n/N}, \tag{6}$$

The $U_n, n = 0, \ldots, N-1$, are complex numbers which can be written as $U_n = |U_n| * \mathrm{e}^{\mathrm{i}\Phi_n}$ with a phase angle $\Phi \in [0, 2\pi)$. According to Parseval the energy of the signal is given by

$$\sum_{n=0}^{N-1} E(n) := \frac{1}{N}\sum_{n=0}^{N-1} |U_n|^2 = \sum_{i=0}^{N-1} |u_i|^2, \tag{7}$$

which yields a connection between the absolute value of U_n and the energy spectrum which is a fundamental quantity in the theory of turbulence: $|U_n| \sim E(n)^{1/2}$. If $E(n)$ is given and one chooses a random angle Φ_n, an inverse Fourier Transform yields obviously a velocity u_k with the prescribed spectrum $E(n)$.

Although the usefulness of this method has been demonstrated for the simulation of a backward facing step [19] or for the DNS of a plane turbulent jet [1,20] it possesses some disadvantages. First, programming

this method is relative complex, because in the three-dimensional case, complicated symmetry conditions for the complex coefficients U_n have to be fulfilled in order to guaranty that the inverse Fourier Transform yields a real field. Different spectra in different coordinate directions add an additional complexity and it is not clear if it is possible to use different spectra at different flow locations. The use of the Fourier Transform leads to some additional restrictions. The grid has to be cartesian and equidistant. The signal which is obtained from the above procedure is periodic. To eliminate this mistake (in axial/temporal direction) the angles Φ_n must be modified by a small amount at random times. If the modification is small, the signal is nearly periodic; if the modification is large, the energy spectrum deviates from the target (see [9]).

A problem which cannot be seen from the above description is that one needs a three-dimensional energy spectrum which is difficult to determine experimentally and rarely done nowadays. In [9] a model spectrum representative for isotropic turbulence has therefore been used,

$$\begin{aligned} &E(\boldsymbol{k}) \sim \ k^4 \exp\left(-2(k/k_0)^2\right) && \text{with the wave number vector } \boldsymbol{k}, \\ &k = \left(k_1^2 + k_2^2 + k_3^2\right)^{1/2} && k_0 = \text{peak wave number}. \end{aligned} \tag{8}$$

Even in the case formula (8) can be regarded as a good approximation of the flow, the question how to choose k_0, cannot be uniquely answered. The biggest disadvantage, but also the most difficult to correct, is the randomness in wave number space. Le and Moin [19] report that in the case of a channel flow simulation 20 boundary layer thicknesses were required to recover the correct skin friction.

We now present a new approach which has some advantages over the above described method. It is based on digital filtering of random data, following the work of [21].

4.2. New concept of inflow data generation: digital filters

Guideline for the development was the practicability, which means that only statistical quantities should be used which can be obtained with reasonable experimental expenses, or alternatively from heuristical estimates. Therefore correlation functions or length scales seem to be adequate alternatives.

In order to create two-point correlations, let r_m be a series of random data with $\overline{r_m} = 0, \overline{r_m r_m} = 1$, then

$$u_m = \sum_{n=-N}^{N} b_n r_{m+n} \tag{9}$$

defines a convolution or a digital linear non-recursive filter. The b_n are the filter coefficients and N is connected to the support of the filter. Because $\overline{r_m r_n} = 0$ for $m \neq n$ if follows easily

$$\frac{\overline{u_m u_{m+k}}}{\overline{u_m u_m}} = \sum_{j=-N+k}^{N} b_j b_{j-k} \Bigg/ \sum_{j=-N}^{N} b_j^2, \tag{10}$$

that means a relation between the filter coefficients and the autocorrelation function of the u_m. Two questions have to be answered: How can this procedure be extended to three dimensions and how is it possible to invert formula (10). By the convolution of three one-dimensional filters one obtains a three-dimensional filter what answers the first question

$$b_{ijk} = b_i \cdot b_j \cdot b_k. \tag{11}$$

To find an answer to the second problem, let's suppose an autocorrelation function is given, i.e. $\overline{u_m u_{m+k}}/\overline{u_m u_m}$. Then it is possible to obtain the coefficients b_n by a multidimensional Newton method. The procedure can be taken from a standard textbook and needs no further comment.

In contrast to the knowledge of the full autocorrelation function one has often an intuitive feeling for the length scale of a flow. Therefore we propose a further simplification, which is especially preferable from an engineering point of view: Instead of $R_{uu}(\boldsymbol{x},\boldsymbol{r})$, where $\boldsymbol{r}$ denotes a distance vector and $r=|\boldsymbol{r}|$, only an integral value, the length scale, should be prescribed. This implies the assumption of a special shape of R_{uu}. For the case of homogeneous turbulence in a late stage, it can be shown [22] that the autocorrelation function takes for a fixed time the form

$$R_{uu}(r,0,0)=\exp\left(-\frac{\pi r^2}{4L^2}\right)\quad\left(\text{with } L=L(t)=\sqrt{2\pi v(t-t_0)}\right). \tag{12}$$

This functional dependance fulfills some basic properties like $R_{uu}(0)=1$, $\lim_{r\to\infty}R_{uu}(r)=0$, and the length scale L can easily be prescribed. In particular an explicit representation of the filter coefficients has been found. Suppose Δx is the grid spacing and $L=n\Delta x$ the desired length scale, then we can write in discretised form

$$\frac{\overline{u_m u_{m+k}}}{\overline{u_m u_m}}=R_{uu}(k\Delta x)=\exp\left(-\frac{\pi(k\Delta x)^2}{4(n\Delta x)^2}\right)=\exp\left(-\frac{\pi k^2}{4n^2}\right) \tag{13}$$

with the filter coefficients

$$b_k\approx\tilde{b}_k\Big/\left(\sum_{j=-N}^{N}\tilde{b}_j^2\right)^{1/2}\quad\text{and}\quad\tilde{b}_k:=\exp\left(-\frac{\pi k^2}{2n^2}\right). \tag{14}$$

Formula (14) is only approximatively valid, but numerically the following error estimate can be given

$$\max_k\left|\exp\left(-\frac{\pi k^2}{4n^2}\right)-\sum_{j=-N+k}^{N}b_j b_{j-k}\Big/\sum_{j=-N}^{N}b_j^2\right|\leqslant 0.001\quad\text{for } N\geqslant 2n \text{ and } n=2,\ldots,100. \tag{15}$$

The last inequality means the support of the filter should be large enough to capture twice the length scale, which anyway makes sense, because otherwise the correlation is truncated to zero before approaching the x-axis.

If a spatial dependence of the b_k is allowed, it is even possible to vary the length scale spatially, simply by applying different sets of filter coefficients at different positions of the grid. For example in a wall bounded flow, the wall normal length scale has to go to zero when approaching the wall. But it must be mentioned that a strong variation of the length scale leads to a deviation of the correlation function from the Gauss shape. The reason is that formula (10) assumes constant filter coefficients. Further distortions can result from Lund's transformation in part 2, but are normally small.

An algorithm for generating inflow data on-the-fly (for equidistant time stepping) may look like this (alternatively one can generate a large volume of data, store it and convect it through the inflow plane by applying Taylors hypothesis):

(a) Choose for each coordinate direction corresponding to the inflow plane a length scale $L_y=n_y\Delta y, L_z=n_z\Delta z$ and also a time scale L_x (or, again by Taylors hypothesis, a length scale). Choose also a filter width according to the condition $N_\alpha\geqslant 2n_\alpha,\ \alpha=x,y,z$ (see (15)).

(b) Initialize and store three random fields $\mathscr{R}_\alpha,\alpha=x,y,z$ of dimensions $[-N_x:N_x,-N_y+1:M_y+N_y,-N_z+1:M_z+N_z]$, where $M_y\times M_z$ denotes the dimensions of the computational grid in the inflow plane.

(c) Calculate the filter coefficients $b(i,j,k)$ according to formulas (14) and (11).

(d) Apply the following filter operation for $j=1,\ldots,M_y,\ k=1,\ldots,M_z$

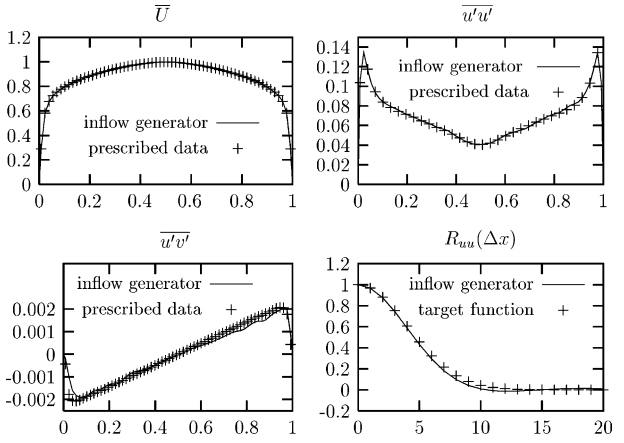

Fig. 2. Validation of the method: plane channel flow.

$$\mathscr{U}_\alpha(j,k) = \sum_{i'=-N_x}^{N_x} \sum_{j'=-N_y}^{N_y} \sum_{k'=-N_z}^{N_z} b(i',j',k')\mathscr{R}_i(i',j+j',k+k'). \tag{16}$$

The result yields the two-dimensional arrays of spatially correlated data $\mathscr{U}_\alpha, \alpha = x, y, z$

(e) Perform the coordinate transformation (formula (5)) resulting in $u_\alpha(j,k)$.

(f) Copy u_α to the inflow plane.

(g) Discard the first y,z-plane of $\mathscr{R}_\alpha$ and shift the whole data: $\mathscr{R}_\alpha(i,j,k) := \mathscr{R}_\alpha(i+1,j,k)$. Fill the plane $\mathscr{R}_\alpha(N_x,j,k)$ with new random numbers.

(h) Repeat the steps (d)–(h) for each time step.

To demonstrate the performance of the method, DNS data of a plane channel flow is prescribed together with an arbitrary chosen correlation function. Fig. 2 shows the validation of the procedure. For reasons of clarity $\overline{v'v'}, \overline{w'w'}$ are omitted from the plots. The results have been averaged over approximately 100 events.

This approach is easily adaptable to experimental data, the length scale can be defined locally for each coordinate direction; the generated signal must not be periodic, but can be; the number of grid points is arbitrary. In addition the method is easy to code.

But it must be mentioned that the new method is also based on the reproduction of statistical data and contains no further physical information. Sometimes we had been asked if the generated velocity field is divergence free. Concerning this point it can be said that in the case of inflow data one cannot speak of divergence because the derivative in axial direction is not defined. Therefore by default our velocity field is not divergence free. But like in [9], it would be easily possible to generate a three-dimensional field and then to perform a projection. Finally this could be convected through the inflow plane using Taylor's hypothesis.

The following section shows in two examples the strong influence of the inflow data on the simulation results and demonstrates the applicability and the usefulness of the new method.

5. Application of the new approach

The first example studies the planar turbulent jet in the Reynolds number range from 1000 to 6000. The simulations are three-dimensional. In the second example we deal with two immiscible fluids in order to

study the mechanisms that lead to primary breakup of a liquid jet. Here the simulations are two-dimensional. The influence of the turbulence on the modulation of the liquid sheet interface is pointed out.

5.1. Direct numerical simulations of plane jets at moderate Reynolds numbers

Turbulent jets have been the subject of experimental and numerical works for over 40 years, because they are often used for the evaluation of physical models. For the axisymmetric jet the very extensive measurements of [23] have been the standard round jet data for a long time. Later it was discovered by using numerical methods, that the far field data of Wygnanski and Fiedler have not satisfied the constraint of the integrated axial momentum equation and that this discrepancy has been due to the semi-confined enclosure [24]. Nearly two decades later detailed measurements with more suitable measurements techniques have been carried out. In contrast to the round jet, according to [24], detailed results newer than those from Gutmark and Wygnangski [25] (denoted GW in the following) are not available for the plane jet, but in view of the above mentioned findings for the axisymmetric jet, the data of GW must be also cast in doubt ([24]). Furthermore, there is little work about free jets at moderate Reynolds numbers.

Many experimental studies use a contraction nozzle and therefore report a top-hat profile for the mean velocity. In combination with the inflow generator this yields a more realistic inflow boundary condition, as we will see below. For the simulations carried out here, velocity profiles with a fluctuation level of 2% have been generated by the procedure presented above. These fluctuations were superimposed to a smoothed top hat profile (17) as in [26]

$$\bar{U} = \frac{U_0}{2} + \frac{U_0}{2}\tanh\left(\frac{z}{2\theta}\right), \tag{17}$$

where θ denotes the shear layer momentum thickness and was set to $D/\theta = 20$ with the nozzle width D. The extension of the computational domain in axial (x), homogenous (y) and vertical (z) direction is $20D \times 8D \times 20D$. The computational domain is resolved with $257 \times 64 \times 512 \approx 8.4 \times 10^6$ grid points, where the nozzle is resolved with 50 cells and the grid is stretched at the lateral boundaries.

Due to the observation, that the distribution of the kinetic energy from the inflow data onto different length scales has an important impact on the evolution of the jet at least in the near field, we studied this influence systematically. Under the assumption that the autocorrelation function has a Gaussian shape, it is now very simple to produce inflow data with different length scales. In Fig. 3 the length scale has been varied in the range from $1/6D, 2/6D, 4/6D$. As perhaps expected the jet spreading rate increases, the more kinetic energy is put into the large scales.

Comparing the axial evolution of the longitudinal fluctuations in Fig. 3 with the random fluctuations in Fig. 1 it is obvious that the data from the inflow generator is much closer to real turbulence.

In the following the far field results for the turbulent jet with $Re = 4000$ are summarized. The length scale at the inflow was set to $1/3D$. The data has been averaged over approximately 10 flow through times based

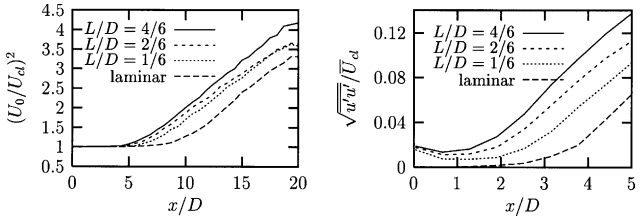

Fig. 3. Influence of different length scales (imposed at the inflow) on the development of a plane jet: velocity decay (left), velocity fluctuations (right).

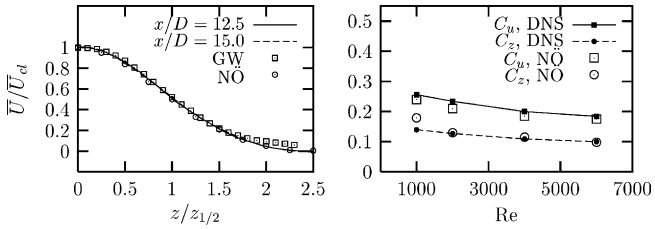

Fig. 4. Normalized axial mean velocity (left). Velocity decay constant C_u and jet spreading rate C_z (right).

on a mean axial velocity. Because the outflow boundary conditions have an upstream influence on the jet, all quantities are evaluated only for $x/D \leqslant 15$. The presented results are normalized with the local centerline velocity U_{cl} and the jet half-width $z_{1/2}$. They are compared with the experimental findings of GW [25] and Namer Ötügen [27], denoted in the following NÖ. As already mentioned, the results of GW for the plane jet, must be cast in doubt at least for the longitudinal fluctuations. Unfortunately in the newer data set of NÖ performed for $Re = 1000$–7000 compared to $Re = 30{,}000$ in GW, the fluctuations $V_{\mathrm{rms}}, W_{\mathrm{rms}}$ as well as the shear stress are not included. This explains the comparison of our simulation results to different data sets.

Fig. 4 (left) shows the axial mean velocity. It is very well represented by a Gaussian profile (18)

$$\frac{U(z)}{U_{\mathrm{cl}}} = \exp\left[- C\left(\frac{z}{z_{1/2}}\right)^2 \right] \tag{18}$$

with $C \approx 0.68$ and agrees well with the data of NÖ. Compared to GW a notable discrepancy is found for $z/z_{1/2} \geqslant 1.5$.

The presented profiles are as usual normalized with U_{cl} and $z_{1/2}$, due to the assumption that the jet reaches a self similar state. Furthermore it is believed that the centerline velocity decays like

$$\left(\frac{U_0}{U_{\mathrm{cl}}}\right)^2 = C_u\left(\frac{x}{D} - C_{u,0}\right) \tag{19}$$

and the jet spreads linearly with x, i.e.

$$\frac{z_{1/2}}{D} = C_z\left(\frac{x}{D} - C_{z,0}\right) . \tag{20}$$

To judge the absolute error it is therefore necessary to compare also the velocity decay constant C_u and the jet spreading rate C_z to experimental data. Fig. 4 (right) shows that over the whole Reynolds number range the agreement is very satisfactory.

For the axial velocity fluctuations shown in Fig. 5 (left), the situation is different. The DNS supports the observation mentioned in [24] that the results of GW were about 20% too high, whereas a good agreement with NÖ was found. Fig. 5 (right) shows the shear stress. Good agreement is also obtained for the other velocity components, not shown here.

5.2. Two-dimensional DNS of primary breakup of a liquid jet

As mentioned above, the atomization can be due to aerodynamic interaction between the liquid and the gas, leading to unstable wave growth on the jet surface, or alternatively the breakup process can start within the nozzle itself and is strongly influenced by turbulence. Probably no single mechanism is responsible.

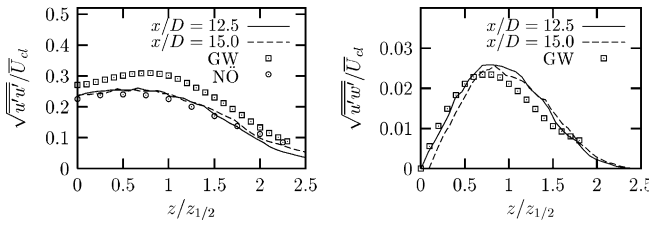

Fig. 5. Normalized longitudinal velocity fluctuations (left). Normalized shear stress (right).

Whereas linear stability analysis can help to understand the first mentioned mechanism (see for example [28]), the influence of turbulence on the disintegration of a liquid jet is more difficult to analyze. In the following we investigate this by generating inflow data with different length/time scales, different fluctuations levels and different mean velocity profiles. The effects of these physical parameters on the modulation of the jet interface in the simulations are compared by means of a Fourier Transform which gives an information about the wavelength on the jet interface and by evaluating the averaged volume concentration $\overline{F}$ which can be regarded as a measure for the deflection of the interface. The extension of the computational domain in axial (x) and vertical (z) direction is here $20D \times 10D$ and is resolved 800×400 grid points. The Reynolds number was set to 4500.

5.2.1. Influence of fluctuation level

To study the influence of the initial fluctuation level on the jet development, we generated velocity data with a velocity profile intermediate between a top hat profile and a fully developed channel flow profile, taken from the measurements of [29], together with a fixed length/time scales and varied only the fluctuation level from 1% to 3%. Experimentally the wavelength can be determined by a Fourier Transform of a greyscale picture, which contains no information about the amplitude of the distortion. Because our data should later be comparable with experimental data we tried to imitate this procedure by eliminating the amplitude from our results, then made a Fourier Transform of this normalized deflection of the interface and averaged over 50 flow-through times. Fig. 6 shows the result. The mean amplitude is plotted over the wavelength in nozzle diameters and it can be clearly seen that the distribution of the energy on different wavelength is constant in all cases. The optimum wavelength is approximately 0.65 nozzle diameters. From the averaged volume concentration function it can be concluded that higher turbulence intensities lead obviously to a stronger excitation.

5.2.2. Influence of different length and time scales

It is more interesting to study now the influence of different energy spectra at the inflow. This can be easily achieved with the inflow generator by varying the length/time scales. The same velocity profile as

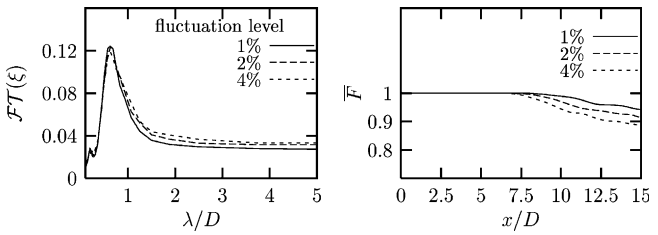

Fig. 6. Influence of the turbulence intensity on primary breakup.

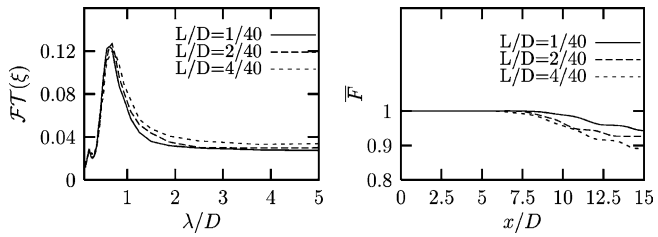

Fig. 7. Influence of different length/time scales on primary breakup.

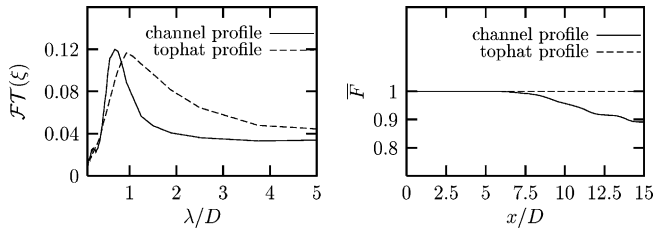

Fig. 8. Influence of different mean velocity profiles on primary breakup.

above has been used. Fig. 7 shows that obviously larger time and length scales lead to a stronger excitation of the jet interface, what can be seen from the averaged volume concentration function, but astonishingly the shape of the spectra is maintained.

5.2.3. Influence of the mean velocity profile

For all investigated cases the mean velocity profile had the most important influence on the modulation of the jet interface. Fig. 8 compares two simulations with a top hat profile and the mean velocity profile described above, respectively. The wavelength for the top hat case is obviously larger compared with the simulation with the channel flow profile, but the excitation of the jet is much stronger in the last case. This is in agreement with the experimental findings of [30] who reported that primary breakup is nearly entirely suppressed, when using a so-called cutter in order to remove the boundary layers of the flow.

6. Conclusions

A new method for generating pseudo turbulent inflow velocities has been developed, tested and applied to two test cases. The method is based on digital filtering of random data and is able to reproduce a prescribed second order (one point) statistic as well as autocorrelation functions. It is easy to implement and provides some advantages over the classical approach using inverse Fourier Transform. In particular this approach is easily adaptable to experimental data, the length scale can be defined locally for each coordinate direction; the generated signal must not be periodic, but can be.

With reference to the plane turbulent jet it is found that the inflow data have a very strong and long living effect on the jet characteristics (here observed until the end of the computational domain). For example the value of the jet spreading rate can reach from 0.8 for a channel flow profile to more than 1.1, using the smoothed top hat profile together with adequate fluctuations. The agreement with experimental findings is very satisfactory and is, in the opinion of the authors, not possible without using the inflow generating procedure.

Concerning the simulation of the liquid sheet, it is possible to study the influencing factor of single properties of turbulence on the evolution of the interface. This is very difficult to achieve experimentally. In fact, if for example the nozzle geometry is changed, in order to obtain a different mean velocity profile, it is probable that also the length scale and turbulence intensities of the flow vary from the original configuration. This makes it difficult to distinguish between different effects. Using the new approach this study has successfully been performed and yielded physically consistent prediction results.

Acknowledgements

The authors are grateful for the financial support by the DFG Schwerpunktprogramm (Fluidzerstäubung und Sprühvorgänge) and SFB 568 (Project A4).

References

[1] M. Klein, A. Sadiki, J. Janicka, Influence of the boundary conditions on the direct numerical simulation of a plane turbulent jet, in: TSFP2, 2nd International Symposium on Turbulence and Shear Flow Phenomena, vol. I, Stockholm, 2001, pp. 401–406.
[2] M. Klein, A. Sadiki, J. Janicka, Influence of the inflow conditions on the direct numerical simulation of primary breakup of liquid jets, in: ILASS-Europe 2001, 17. Annual Conference on Liquid Atomization and Spray Systems, Zürich, 2001, pp. 475–480.
[3] S. Stanley, S. Sarkar, Influence of nozzle conditions and discrete forcing on turbulent planar jets, AIAA J. 38 (2000) 1615–1623.
[4] T. Lund, X. Wu, D. Squires, Generation of turbulent inflow data for spatially-developing boundary layer simulations, J. Comp. Phys. 140 (1998) 233–258.
[5] P. Moin, K. Mahesh, Direct numerical simulation, a tool in turbulence research, Ann. Rev. Fluid Mech. 30 (1998) 539–578.
[6] P. Spalart, Direct numerical simulation of a turbulent boundary layer up to $Re_\theta = 1410$, J. Fluid Mech. 187 (1988) 61–98.
[7] M. Lygren, H. Andersson, Influence of boundary conditions on the large scale structures in turbulent plane couette flow, in: S. Banerjee, J. Eaton (Eds.), Turbulence and Shear Flow, vol. 1, Begell House, 1999, pp. 15–20.
[8] B. Rembold, N. Adams, L. Kleiser, Direct numerical simulation of a transitional rectangular jet, in: TSFP2, 2nd International Symposium on Turbulence and Shear Flow Phenomena, vol. I, Stockholm, 2001, pp. 55–60.
[9] S. Lee, S. Lele, P. Moin, Simulation of spatially evolving compressible turbulence and the application of taylors hypothesis, Phys. Fluids A 4 (1992) 1521–1530.
[10] P. Druault, E. Lamballais, J. Delville, J.-P. Bonnet, Development of experiment/simulation interfaces for hybrid turbulent results analysis via the use of DNS, in: TSFP2, 2nd International Symposium on Turbulence and Shear Flow Phenomena, vol. II, Stockholm, 2001, pp. 5–14.
[11] B. Lafaurie, C. Nardonne, R. Scardovelli, S. Zaleski, G. Zanetti, Modelling merging and fragmentation in multiphase flows with surfer, J. Comp. Phys. 113 (1994) 134–147.
[12] M. Klein, A. Sadiki, J. Janicka, Effects of the surface stretching or the surface deformation rate on the breakup of a viscous drop in simple shear flow: numerical simulation, in: 5th International Symposium on Engineering Turbulence Modelling and Measurements, Mallorca, September 2002.
[13] R. Scardovelli, S. Zaleski, Direct numerical simulation of free surface and interfacial flows, Ann. Rev. Fluid Mech. 31 (1999) 567–603.
[14] D. Gueyffier, A. Nadim, J. Li, R. Scardovelli, S. Zaleski, Volume of fluid interface tracking with smoothed surface stress methods for three-dimensional flows, J. Comp. Phys. 152 (1999) 423–456.
[15] P. Sagaut, Large Eddy Simulation for Incompressible Flows, Springer, Berlin, 1998.
[16] M. Klein, A. Sadiki, J. Janicka, Direct numerical simulations of plane turbulent jets at moderate Reynolds numbers, in: 20th IUTAM Congress, ICTAM 2000, Chicago, 2000.
[17] C. Mengler, C. Heinrich, A. Sadiki, J. Janicka, Numerical prediction of momentum and scalar fields in a jet in cross flow: comparison of les and second order turbulence closure calculations, in: TSFP2, vol. II, Stockholm, 2001, pp. 425–430.
[18] A. Lefebvre, Atomization and Sprays, Taylor & Francis, London, 1989.
[19] H. Le, P. Moin, Direct numerical simulation of turbulent flow over a backward-facing step, Tech. Rep. TF-58, Standford University, 1994.
[20] S. Stanley, S. Sarkar, J. Mellado, A study of the flow field evolution and mixing in a planar turbulent jet using direct numerical simulation, J. Fluid Mech. 450 (2002) 377–407.
[21] H. Nobach, Verarbeitung stochastisch abgetasteter signale, Ph.D. Thesis, Universität Rostock, 1997.

[22] G. Batchelor, The Theory of Homogeneous Turbulence, Cambridge University Press, Cambridge, 1953.
[23] I. Wygnanski, H. Fiedler, Some measurements in the self-preserving jet, J. Fluid Mech. 38 (1975) 577–612.
[24] J. Bonnet, R. Moser, W. Rodi, AGARD advisory report 345, A Selection of Test Cases for the Validation of Large Eddy Simulations of Turbulent Flows, AGARD 1998, 7 Rue Ancelle, 99200 Neuilly-sur Seine, France, 1998, Ch. 6.3 Jets, p. 35.
[25] E. Gutmark, I. Wygnanski, The planar turbulent jet, J. Fluid Mech. 73 (1976) 465–495.
[26] C.L. Ribault, S. Sarkar, S. Stanley, Large eddy simulation of a plane jet, Phys. Fluids 11 (1999) 3069–3083.
[27] I. Namer, M. Ötügen, Velocity measurements in a plane turbulent air jet at moderate Reynolds numbers, Exp. Fluids 6 (1988) 387–399.
[28] X. Li, Spatial instability of plane liquid sheets, Chem. Eng. Sci. 48 (1993) 2973–2981.
[29] K. Heukelbach, C. Tropea, Influence of the inner flowfield of flat fan pressure atomizers on the disintegration of the liquid sheet, in: ILASS-Europe 2001, 17. Annual Conference on Liquid Atomization and Spray Systems, Zürich, 2001, pp. 613–618.
[30] P. Wu, R. Miranda, G. Faeth, Effect of initial flow conditions on primary break-up of nonturbulent and turbulent liquid jets, Atomization and Sprays 5 (1995) 175–196.